ISSN: 0975-3583, 0976-2833 VOL12, ISSUE06, 2021

Based on Sparse Representation and Feature Extraction in Clinical Image Fusion

B. Bhaskar Reddy[1], P. Imran Khan[2], Dr. B. Dhananjaya[3]
Professor[1,3], Assistant Professor[2]
Department of Electronics and Communication Engineering
Bheema Institute of Technology and Sciences, Adoni-518301.[1,2,3]

Abstract: There are several advantages to using minimal depiction in a narrative multi-scale geometric assessment contraption over normal image depiction methods. Regardless, the typical poor representation fails to consider the unique structure and the time-multifaceted architecture. To address all of these difficulties at the same time, a novel blend segment for multimodal clinical images relying on poor depiction and decision direct is now being considered. In order to save more essentiality and edge information, three decision maps are organised, including the structure information map (SM) and the essentialness information map (EM). For example, SM has the local structure that is derived from a Gaussian Laplacian (LOG) and it also contains the essentiality and imperativeness movement characteristic that is defined by the mean square deviation (EM). In order to speed up computations, decision control is introduced to the depiction-based technique. More structure and imperativeness information may be extracted from source images using this proposed method, which further enhances the notion of the combined results. According to the results of 36 studies including CT/MRI, MR-T1/MR-T2, and CT/PET images, the technique subject to SR and SEM outmanoeuvres five of the most advanced approaches..

1. Introduction

Medical imaging attracts more and more attention due to the increasing requirements of clinic investigation and disease diagnosis. Owing to different imaging mechanisms, medical images of different modals provide a variety of complementary information about the human body in a limited domain. For example, the computed tomography (CT) images provide better information on dense tissue, the positron emission tomography (PET) images supply better information on blood flow and tumor activity with low space resolution, and the magnetic resonance (MR) images show better information on soft tissue. Moreover, the MR-T1 images give more detailed information about anatomical structures, whereas the MR-T2 images contain a greater contrast between the normal and abnormal tissues [1–4]. However, single multiple modality cannot satisfy the demand of images with highresolution and visualization for disease diagnosis.

In this regard, medical image fusion is a useful and powerful technique for integrating complementary information from multimodality images to improve the diagnostic accuracy. Besides, the fused images are more suitable for assisting the doctors in diagnosis and treatment planning [5]: fusing MR and CT images can generate the images which can describe the soft tissue and bone in order to concurrently represent anatomical and physiological features of the human body [6, 7]. MR-T1 and MR-T2 images are fused to segment white matter lesions and guide neurosurgical resection of epileptogenic lesions [7, 8]. In oncology, the combined PET/CT imaging is helpful to view the anatomical, physiological characteristics and the tumor activity [9,10]. More than that, medical image fusion not only helpsin diagnosing diseases but also reduces the storage cost [8].As the most popular technique of the image fusion, theMultiscaledecompositionmethods have developed quickly inrecent years, such as discrete wavelet transform(DWT) [3, 7],

The main contribution of this paper is as follows:

(1) To add the local structure and energy information ofthe source images into the SR algorithm for medicalimage fusion, we design three decision maps toextract the local energy and structure features of thesource images.

(2) It is good to use the decision to reduce the number ofimage blocks to sparse representation, so that we canget the results in much shorter time. Using the mapsto remain more structure and energy informationin fused images will also improve the quality of theresults.

ISSN: 0975-3583, 0976-2833 VOL12, ISSUE06, 2021

2. The Framework of the Proposed Method

There is the framework of the proposed approach based on SR and feature extraction as shown in Figure 1.we divide all source images$A$and B with the size of $m\times n$ into patches yi,j 1 and yi,j 2 through a sliding window with the size of$\times w(i \le m-w, j \le n-w)$. All patches are arranged into vectors $(i-1)*(n-w)+j$ 1 and $V(i-1)*(n-w)+j$ 2 from left to right and from top to bottom. Secondly, we group these vectors into vector pairs according to corresponding positions of original patches and design the decision map according to their features separately. Thirdly, we use the decision map to determine which one vector of each group as the result when the map is marked as 1 or 2. It means that these groups are regarded as the input of the sparse representation system when the map is marked 0. Fourthly, we fuse the other vector pairs by the SR method. Finally, the system can generate the fused results according to the decision map. The overlaps of the patches are averaged.

2.1. SR. In SR algorithms, a signal can be expressed as a sparsecombination of the fewest possible atoms of an overcompletedictionary [29]. Let $V\in Rm$ denote a signal vector fromthe source images and let $D\in Rm\times k$ $(k>m)$ denote anovercomplete dictionary whose column vectors are its atoms.Thesignal vector can be represented as$V = D\theta$, where$\theta\in Rk$is a sparse coefficient vector. The sparse coefficient vector isacquired by solving the following question:

$$\begin{aligned} \widehat{\theta} = \arg\min_{\theta} \quad & \|\theta\|_0 \\ \text{s.t.} \quad & \|V - D\theta\|_2^2 \le \varepsilon, \end{aligned} \tag{1}$$

2.2. The EnergyMap and the StructureMap. Let us regard $yi,1$and$yi,j2$ as mean values of $yi,j1$ and yi,j 2 , respectively. We use$\|yi,1\|2$ as the sign of energy and the mean square deviation$(1/64)\|yi,j1 - yi,j1\|2$ as the sign of energy distribution for $yi,j1$,which are similar to $yi,j2$. We design the first decision mapEM$\in RM\times N$ (where$M = m- w$ and $N = n - w$) whichcalled the energy map by

$$t1 = \frac{1}{64}\left(\left\|y_1^{i,j}\right\|_2 - \left\|y_2^{i,j}\right\|_2\right),$$

$$t2 = \frac{1}{64}\left(\left\|y_1^{i,j} - \overline{y}_1^{i,j}\right\|_2 - \left\|y_2^{i,j} - \overline{y}_2^{i,j}\right\|_2\right),$$

3. Experiments

To evaluate the performance of the proposed method, three experiments are implemented. All the images are the same size of 256 × 256 pixels. In this paper, we train the dictionary with K-SVD using the pictures as shown inFigure 3.The error tolerance ε is set to be 0.01.The maximum iterations of the K-SVD are set to be 30. The initial dictionary is the DCT dictionary with the size of 64 × 256.We use OMP to estimate the sparse coefficients for simplicity. The moving step of the sliding window is set to be one pixel. We use three kinds of medical image pairs including CT/MR images, MR-T1/MRT2 images, and CT/PET images to test the performances of those abovementioned methods. The DCT dictionary and trained dictionary are shown in Figure 4. The window size of LOG is set to be 5 × 5, and σ is set to be 2.

For comparison, five state-of-the-art methods are evaluated in the experiments, including methods based on NSCT[1, 6], method based on JSR [12], and methods based on NSCT and SR [15, 18]. In this paper, five objective evaluation measurements parameters are adopted to evaluate the fusion performance. There is local quality index $(Q0)$ [34], weighted fusion quality index (QW) [34], edge-dependent fusion quality index (QE) [34], QAB/F [35] which measures the transmission of edge and visual information from source images to fused images, and mutual information (MI) [36] which computes the information transformed from the source images to the fused images. For $Q0$, QW, QE, and QAB/F, they all lie in the interval

ISSN: 0975-3583, 0976-2833 VOL12, ISSUE06, 2021

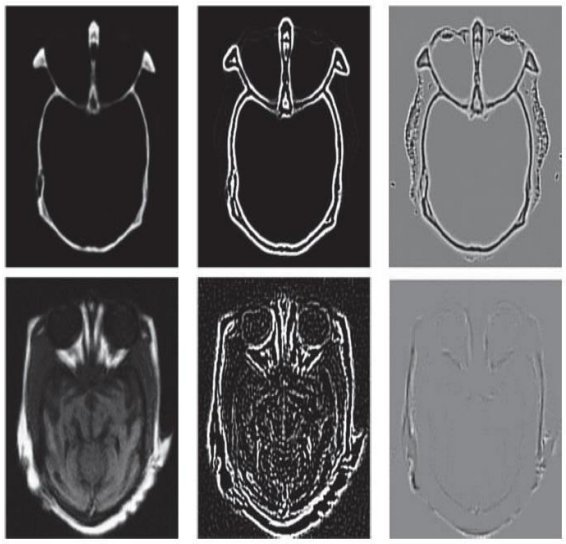

(a) (b) (c)

Figure 2: (a)The source images, (b) the structure information of LOG, and (c) the local structure information normalization.

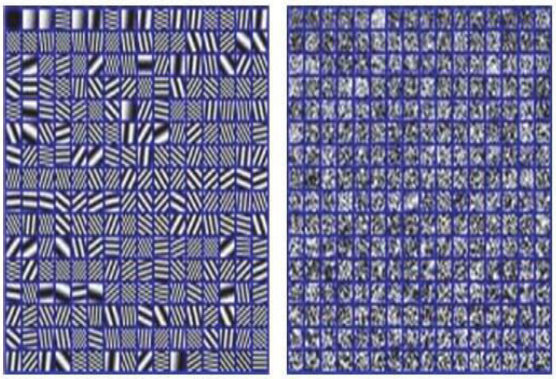

Figure 4: The DCT dictionary and the trained dictionary

experiments are carried out in the PC with the Intel i7-3770 CPU 3.40GHz and 4G RAM, operating under MATLAB R2010a.3.1.The CT Images andMR Images Fusion. In the first experiment,the CT and MR images are fused with eight differentimage fusion methods listed above. We used 12 groups CTand MR images to test the performance of these methodsas shown in Figure 3. Two groups of results are shown in
Figure 5. It is obviously seen that the results of NSCT arefuzzy in some parts, especially in Figures 5(m) and 5(n),the results of SR + NSCT [15], SR + SM, and SR + SEMcan reserve better source image boundary information thanthe results of the other methods. And these results have noblock effects because all the methods use the sliding windowstrategy, in which NSCT [1] and NSCT [6] use the windowwith size of 3 × 3 and the others use the window with size of8 × 8. And results of NSCT [1], NSCT [6], JSR [12], and SR+ NSCT [18] are brighter than all source images, which willlead some dim information to be hidden by light information.
As shown in Figures 5(m), 5(n), 5(o), and 5(q), we cannottell the tissue information between the skull and brain. In acertain extent, the proposedmethod can ease these problemsand meanwhile remain the merits of the SR based methods.Comparatively, the results of SR + SEM can remain better image boundary and energy information, where we can getbetter anatomical information fromCT images and soft tissueinformationfromMRimagessimultaneously. More than that,the calcified meningioma in Figure 5(f) can be distinguishedfrom background easily in Figures 5(r), 5(s), and 5(t).

ISSN: 0975-3583, 0976-2833 VOL12, ISSUE06, 2021

3.2. The MR-T1 and MR-T2 Images Fusion. In the second experiment, we used 12 groups MR-T1 and MR-T2 images to test the performance of these methods as shown in Figure 3. To illustrate the proposed fusion method, two sets of results are presented in Figure 6. In general, the results of NSCT [1], NSCT [6], and SR + NSCT [18] look gloomy and bright, demonstrating the grey distortion happens. NSCT [1], NSCT
[6], JSR [12], and SR + NSCT [18] create many bad edges and make the fused results too smoothness. Comparatively, the results of SR + NSCT [15] and proposed methods show better boundary information and energy information with fewer artifacts, so that we can get better information on adipose tissue from MR-T1 images and information on vascular and tumor fromMR-T2 images. Compared to the other methods, the results of proposed methods contain more information from the source images. The proposed methods preserve both better local edge and texture information, which is the vital information for diagnosis. The sub acute premature hematoma is seen clearly in Figure 6(l), and we can see the location and contour of the intracranial hematoma in Figures 6(r), 6(s), and 6(t). For 12 MR-T1 and MR-T2 fused results, the average scores of quantitative evaluation metrics are listed in Table 2 and the "bold" values indicate the highest values.

Table 1:The objective evaluation and running time for CT and MR image fused results of all methods.

	Q_0	Q_W	Q_E	$Q_{AB/F}$	MI
NSCT [1]	0.5960	0.7511	0.5707	0.5857	4.6665
NSCT [6]	0.5958	0.7554	0.5793	0.5892	4.6711
JSR [12]	0.6493	0.8148	0.6296	0.5838	3.6120
SR + NSCT [15]	0.6611	0.8477	0.6249	0.6447	4.0421
SR + NSCT [18]	0.6527	0.8161	0.5572	0.5866	3.6371
SR + SM	0.6566	0.8466	0.6992	0.6630	4.5467
SR + EM	0.6643	0.8355	0.6919	0.6477	4.2687
SR + SEM	**0.6679**	**0.8477**	**0.7043**	**0.6677**	**4.6721**

Table 2:The objective evaluation and running time for MR T1 and MR T2 image fused results of all methods.

	Q_0	Q_W	Q_E	$Q_{AB/F}$	MI
NSCT [1]	0.6311	0.8178	0.6166	0.6374	5.4548
NSCT [6]	0.6316	0.8202	0.6192	0.6387	5.4252
JSR [12]	0.6732	0.8369	0.6367	0.5744	3.9141
SR + NSCT [15]	0.6896	0.8543	0.6313	0.6608	4.8713
SR + NSCT [18]	0.6741	0.8385	0.5563	0.5774	3.9210
SR + SM	0.6832	0.8520	0.7029	0.6676	5.3846
SR + EM	0.6911	0.8542	0.6989	0.6577	4.9104
SR + SEM	**0.6991**	**0.8558**	**0.7063**	**0.6746**	**5.4563**

Table 3:The objective evaluation and running time for CT and PET image fused results of all methods.

	Q_0	Q_W	Q_E	$Q_{AB/F}$	MI
NSCT [1]	0.5083	0.9442	0.7297	0.7783	4.8657
NSCT [6]	0.5132	0.9475	0.7414	0.7862	4.9470
JSR [12]	0.4988	0.9590	0.8095	0.7558	3.5924
SR + NSCT [15]	0.4983	0.9635	0.7628	0.7863	4.0568
SR + NSCT [18]	0.5046	0.9612	0.7564	0.7625	3.6635
SR + SM	0.4992	**0.9652**	0.8337	0.8030	4.7986
SR + EM	**0.5234**	0.9642	0.8311	0.7984	4.5778
SR + SEM	0.5100	**0.9652**	**0.8369**	**0.8041**	**4.9720**

3.3. The CT Images and PET Images Fusion. In the thirdexperiment, we used 12 CT and PET image pairs to testthe performance of these methods as shown in Figure 3.Two sets of results are shown in Figure 7. Comparatively,the results of NSCT [1] and NSCT [6] are best especially inenergy information, so that the fused images can capture bothmore spatial information in the CT images and functionalinformation contents in PET images. However, in clinicalapplications, doctors need to see the position of bone andtumor to determine pathology and aid in diagnosis.

ISSN: 0975-3583, 0976-2833 VOL12, ISSUE06, 2021

Theresults fused by SR + SEMcontainmore detailed informationand higher contrast but without information distortion sothat we can see the outline of the kidney clearly in Figures7(r), 7(s), and 7(t). Nasopharyngeal carcinoma can be seenin Figure 7(b), and we can use the result fused by proposedmethod to locate it in Figure 7 SR+NSCT[15], SR + SM, andSR + SEM easily, where are helpful to view the tumor activity,allowing physicians to better understand the effect of cancertreatment

3.4. The Time Complexity Analysis. To realize the fusionand reconstruction of 3D medical images, a lot of CT/PETand MR/PET image slices need to be fused firstly [37, 38].Therefore, there is a need to find a faster and stronger image fusion algorithm. As shown in Figure 8,we record the averagetime consumption of different methods for 36 differentmedical image pairs listed. It is evident that the multiscaleapproaches including NSCT [1] and NSCT [6] are very fastwhile the SRbased approaches (JSR [12], SR+NSCT [15], andSR +NSCT [18]) takemuch more time. Comparably, the timeconsuming of SR + SM is about 1/20, SR + EM is about 1/20,and SR + SEM is about 1/50 of the SR based approach. Fromthe above analysis and discussion, we draw the conclusionthat SR + SEM outperforms all the others in the field ofmedical image fusion. Because it contains more originalinformation from source images and better local structureinformation, our methods are more appropriate for doctorsto localize the abnormal masses and tumors in patients.

4. Conclusion

It is suggested in this research that a novel method of medical picture fusion be developed using SR and feature extraction. As opposed to the current standard SR-based fusion approaches, there are at least three important enhancements To begin, we developed three decision maps for enhancing the quality of SR-based image fusion algorithms for extracting structural and energetic information from the source pictures. [*] This method may assist preserve as much of the original information as possible from the source photos. SR-based approaches get a performance boost with the inclusion of a decision map. The suggested methodology requires just 1/50 of the time required by the typical SR method to achieve the picture fusion. Third, the quality of the merged findings is vastly improved by including the structure and energy information from the source pictures into the decision map. It seems that the suggested fusion methodology can outperform existing fusion approaches both subjectively and objectively.

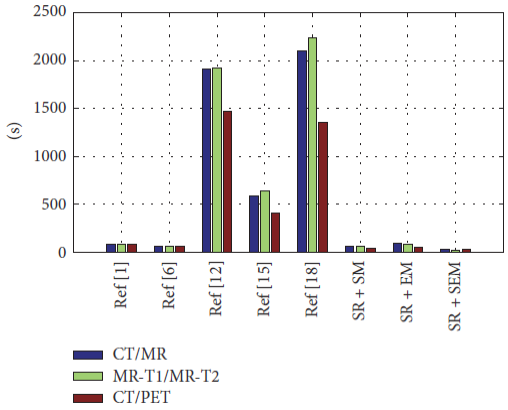

Figure 8: The time consuming of different fusion methods.

References

[1] P. S. Gomathi and B. Kalaavathi, "Multimodal medical imagefusion in non-subsampled contourlet transform domain," Circuits& Systems, vol. 7, no. 8, pp. 1598–1610, 2016.

[2] M. D. C. Vald´esHern´andez, K. J. Ferguson, F.M. Chappell, andJ. M. Wardlaw, "New multispectral MRI data fusion techniquefor white matter lesion segmentation: method and comparisonwiththresholding in FLAIR images," European Radiology, vol.20, no. 7, pp. 1684–1691, 2010.

[3] Z. Liu, H. Yin, Y. Chai, and S. X. Yang, "A novel approach formultimodal medical image fusion," Expert Systems with Applications,vol. 41, no. 16, pp. 7425–7435, 2014.

[4] Y. Yang, S.Tong, S. Huang, andP.Lin, "Log-Gabor energy basedmultimodal medical image fusion in NSCT domain," Computationaland Mathematical Methods in Medicine, vol. 2014,Article ID 835481, 12 pages, 2014.

[5] V. D. Calhoun and T. Adali, "Feature-based fusion of medicalimaging data," IEEE Transactions on Information Technology inBiomedicine, vol. 13, no. 5, pp. 711–720, 2009.

ISSN: 0975-3583, 0976-2833 VOL12, ISSUE06, 2021

[6] P. Ganasala and V. Kumar, "CT and MR image fusion schemeinnonsubsampledcontourlet transform domain," Journal ofDigital Imaging, vol. 27, no. 3, pp. 407–418, 2014.
[7] R. Shen, I. Cheng, and A. Basu, "Cross-scale coefficient selectionfor volumetric medical image fusion," IEEE Transactionson Biomedical Engineering, vol. 60, no. 4, pp. 1069–1079, 2013.
[8] Z. Wang and Y. Ma, "Medical image fusion using m-PCNN,"Information Fusion, vol. 9, no. 2, pp. 176–185, 2008.
[9] G. Bhatnagar, Q. M. Jonathan Wu, and Z. Liu, "Human visualsysteminspiredmulti-modalmedical image fusion framework,"Expert Systems with Applications, vol. 40, no. 5, pp. 1708–1720,2013.
[10] L. Yang, B. L. Guo, and W. Ni, "Multimodality medical imagefusion based on multiscale geometric analysis of contourlettransform," Neurocomputing, vol. 72, no. 1-3, pp. 203–211, 2008.
[11] M. Kim, D. K. Han, and H. Ko, "Joint patch clustering-baseddictionary learning for multimodal image fusion," InformationFusion, vol. 27, pp. 198–214, 2016.
[12] Y. Yao, P. Guo, X. Xin, and Z. Jiang, "Image fusion by hierarchicaljoint sparse representation," Cognitive Computation, vol. 6,no. 3, pp. 281–292, 2014.
[13] T. Guha and R. K. Ward, "Learning sparse representationsfor human action recognition," IEEE Transactions on PatternAnalysis and Machine Intelligence, vol. 34, no. 8, pp. 1576–1588,
2012.
[14] S. T. Li, H. T. Yin, and L. Y. Fang, "Group-sparse representationwith dictionary learning for medical image denoisingandfusion," IEEE Transactions on Biomedical Engineering, vol. 59,
no. 12, pp. 3450–3459, 2012.
[15] Y. Liu, S. Liu, and Z. F. Wang, "Medical image fusion by combiningnonsubsampledcontourlet transform and sparse representation,"in Pattern Recognition, vol. 484 of Communicationsin Computer and Information Science, pp. 372–381, Springer,Berlin, Germany, 2014.
[16] H. Yin, S. Li, and L. Fang, "Simultaneous image fusionand super-resolution using sparse representation," InformationFusion, vol. 14, no. 3, pp. 229–240, 2013.